Spatial Modeling of Potential Zones for Groundwater and Their Spatial Overlap with Used and Covered Land in Western Basrah Province Using AHP and ArcGIS

Issam Mohammed Ali Alradiny, Ammar Dakhil and Ayman A. Hassan

Abstract: *Given the worsening scarcity and pollution of surface water, particularly in southern Iraq's Basrah Governorate, with its arid desert environment and scarce rainfall, the importance of utilizing groundwater, especially for agricultural and domestic uses, becomes evident. In order to make optimal use of groundwater, decision-makers should be provided with systematic scientific studies on this water resource so that it can be managed properly. The Analytic Hierarchy Process method (AHP) was utilized to find groundwater potential zones (GWPZ), as well as the (ArcGIS Pro) software environment with addition to remote sensing. The area for this study was located in Basrah in southern Iraq, and it covered an area of 132.662 km2. Thematic layers were essential to the study and five of them were used according to their importance in the previously mentioned area, and they are: groundwater's depth, LULC, slope, drainage density and rainfall. These parameters results were identified to create a map of potential groundwater locations for the study, and this was done through the use of a pairwise comparison matrix. The consistency ratio analysis (CR) illustrated that the previous inferred results are reliable and suitable to map zones where groundwater could potentially be found, as it was shown to be 0.022. Additionally, these same findings identified that the groundwater's depth was the most influential parameter, as it had a relative weight of 0.4875, after which comes the LULC parameter which has weight of relatively 0.2277, whereas the lowest recorded weight was the of rainfall's as it had a*

Issam Mohammed Ali Alradiny
E-mail: issam.abdalkareem@uobasrah.edu.iq
Department of Civil Engineering, College of Engineering, University of Basrah, Iraq
Ammar Dakhil
Email: ammar.dakhil@uobasrah.edu.iq
Department of Civil Engineering, College of Engineering, University of Basrah, Iraq
Ayman A. Hassan
ayma.alk@uobasrah.edu.iq
Department of Civil Engineering, College of Engineering, University of Basrah, Iraq

value of only 0.0556 due to the low rainfall and limited spatial variation in the region. The results, after dividing the map into five categories, showed that approximately one third of the specified area for the study (30.61%) had high groundwater potential zones. On the other hand, zones with potentially very high and medium amount of groundwater covered 26.56% and 17.23% of the area. Meanwhile, zones with potentially low and very low groundwater covered only 17.43% and 8.17%, respectively. To confirm the accuracy of the study model, field validation was conducted using 10 well sites, revealing an 80% accuracy rate. Statistical analysis of the study results revealed a strong positive correlation between agriculture and grasses practices and groundwater potential zones. These two activities are usually found together at a high percentage in zones with very high and high potential for groundwater, measuring 97.31% and 85.25% In contrast, the results of the statistical analysis showed an inverse relationship between barren land and the potential of groundwater. As for the urban area, the results revealed that it peaks in areas of medium potential and recedes in areas of very high potential. The study concluded by proposing 26 future well-drilling sites in high and very high potential areas, which provides a means to help decision-makers manage groundwater in the best way and achieve the desired development.

Keywords: Basrah, Analytic Hierarchy Process (AHP), Groundwater Potential Zone (GWPZ), Land Use and Land Cover (LULC)

Introduction

The world is currently experiencing a severe water crisis, with studies indicating that approximately 4 billion people face acute water scarcity annually (Mekonnen & Hoekstra, 2016). This scarcity is exacerbated by the catastrophic increase in surface water pollution, with about 48% of global sewage being discharged into rivers and water bodies without treatment, rendering them unsuitable for human and agricultural use (Jones et al., 2021). Locally, Iraq is on the brink of a genuine water disaster. Both the Tigris and Euphrates rivers have experienced a decrease in the amount of water that flows in them when compared to pre-1975 levels (Metwally et al., 2024). This deficit, coupled with low rainfall, has led to the desertification of vast areas and severely damaged the agricultural sector, which is the primary source of income for a large percentage of the population (Asaad & Abed, 2020; Al-Ansari, 2021).

Faced with this quantitative and qualitative decline in surface water, groundwater has emerged as a successful alternative and an indispensable safety valve for achieving water and food security. It is characterized by the presence of geological layers that act as natural purification filters and high resistance to high evaporation rates (Lall et al., 2020). Globally, groundwater meets 50% of drinking water needs and about 43% of agricultural requirements (Bierkens & Wada, 2019). European countries rely on it to secure 75% of their drinking water, while it constitutes the primary source for 50% of water in Arab countries, most of which are on the brink of drought (Hindiyeh et al., 2023).

This importance is particularly evident in Basrah Governorate in southern Iraq, which suffers from a severe water crisis that peaked after the hydrological collapse of the Shatt al-Arab in 2018 due to a shortage of freshwater releases (Ahmed & Al-Zewar, 2020; Al-Asadi & Alhello, 2019; Mawat & Hamdan, 2024). Total dissolved solids (TDS) concentrations exceeded 15,000 mg/L in the city center, reaching 37,620 mg/L in downstream areas (Al-Mahmood & Mahmood, 2019; Abdullah, 2024), leading to a near-zero efficiency in water treatment plants (Al Saad & Hamdan, 2020; Almuktar et al., 2020; Faroon et al., 2023; Mahdi & Hamdan, 2022).

Faced with the dual challenges of pollution in the Shatt al-Arab and inadequate infrastructure, investing in the Dibdibah aquifer on the western side of Basra has become an inevitable and sustainable option, in stark contrast to the alluvial plain aquifer, which suffers from high salinity and severe pollution (Jassim & Goff, 2006; Dawood, Khudier, et al., 2018; Al-Mallah et al., 2022; Al-Qurnawy et al., 2024). The Dibdibah aquifer is characterized by its high hydrogeological properties and permeability, making it efficiently used for agriculture in the Zubair and Safwan regions (Al Aboodi & Munshid, 2017; Al-Mallah et al., 2022). However, excessive agricultural expansion is placing increasing pressure on the aquifer, making it vulnerable to depletion and degradation without proper management (Al-Mallah et al., 2022; Alqurnawy et al., 2022).

The first step in protecting and managing the aquifer is the accurate identification of groundwater potential zones (GWPZs). Instead of traditional methods such as geophysical surveys and random drilling, which are time-consuming, labor-intensive, and costly (Sander et al., 1996; Jha et al., 2010), other methods have proven themselves to be efficient in producing accurate maps in the southern Iraqi environment such as multi-criteria analysis (MCDM), remote sensing (RS), and geographic information systems (GIS), achieving these results with lower cost and less effort (Al-Qurnawy et al., 2024; Al-Abadi & Al-Qurnawy, 2021; Al-Abadi et al., 2016). In this context, a reliable method was found for assigning accurate scientific weights to influential parameters, such as the analysis hierarchy model (AHP), which informs whoever is responsible for making decisions towards efficient management (Saravanan et al., 2021; Aykut, 2021).

Given the urgent need to manage the Dibdibah aquifer efficiently in light of the collapse of surface water, the goal of the study became finding groundwater potential zones (GWPZ) by using RS, AHP model, and GIS. It also seeks to establish a quantitative and spatial correlation between GWPZ and LULC, and to provide scientific proposals for optimal locations for new wells. These proposals will serve as a tool for decision-makers, assisting them in planning, managing, and sustaining the aquifer for future generations.

Materials and Methods

2-1 Study Area

The location of the study area was in southern Iraq, in Basrah Governorate, between latitudes 30° 29′ 30″N and 30° 38′ 43″N and longitudes 47° 4′ 39″E and 46° 54′ 12″E, with an area of 132.6617 km². The Al-Lahis area is located in western part of Basrah Governorate, 105 km from the governorate's center. It is bordered to the east by the alluvial plain, the edges of the Al-Hammar Marsh, and Al-Madina District. To the left, it is bordered by the vast expanses of the southern desert extending to Samawah Governorate, and to the north by the desert edges of Nasiriyah Governorate. The Al-Lahis area differs from the eastern and northern areas of Basrah Governorate (Al-Qurna, Al-Madina, and the center). The governorate is considered unsuitable for agricultural or urban development because these areas lie within the alluvial plain and are characterized by shallow, highly saline groundwater within the Quaternary deposits (Al-Jiburi & Al-Basrawi,2011). In contrast, the Al-Lahis area, which represents a geological transition zone, is relatively high desert land belonging to the western plateau in the southern Badia (where it serves as a natural drainage zone for groundwater). This area descends to the very low-lying lands that constitute the alluvial plain and marshes (Hussain et al., 2021). Geologically and hydrologically, this area is considered a transition zone and a natural drainage zone (Albhadili et al., 2023). Therefore, the Al-Lahis area is considered the eastern edge of the western plateau, which is characterized by containing the Dibdibah aquifer. The Dibdibba Aquifer has high permeability (Al-Sudani, 2019).

The selection of this study area is driven by its significant agricultural expansion over the past two decades, making it a crucial hub for modern agricultural investment in Basrah. Despite the agricultural sector's vital role in sustainable development at both regional and national levels, this area lacks adequate hydrogeological studies. Therefore, there is an urgent need for detailed field investigations to support its rapid development**.** The administrative and geological boundaries, topography, and sampling sites all contributed in identifying an area with triangular borders to be the study area. Separating the water basins was a major priority for the integrity of the study results, as the water reservoir for this area is part of the Al-Dabdaba Formation aquifer, while several kilometers to the east and north of this area there is another reservoir belonging to the alluvial plain. The factor of overlapping administrative boundaries also contributed to determining the shape of the study area, as this area is only several kilometers away from the edges of Al-Nasiriyah Governorate. In addition, to the left of the study area there are rugged terrain and barren lands. The distribution of the sampling sites for the study wells and monitoring wells also contributed to determining the boundaries of this area and making it take this shape.

The study area (Al-Lahis) is characterized by a homogeneous geological formation known as the Dibdibba Formation, which lies within the stable shelf zone according to the tectonic and geological classifications of Iraq (Jassim & Goff, 2006). This formation represents the main shallow aquifer in the region. The soil in the area is characterized by loam soil, meaning it is a mixture of sand, silt, and clay, giving it ideal physicochemical properties for many agricultural uses. Topographically, the study area is predominantly flat with an elevation of 14-22 m above sea level (Abdulameer et al., 2018; Al-Kaaby & Albadran, 2020; Al-Sudani, 2019; FAO, 2003)

Basrah Governorate is one of the hottest regions in the world, especially during the summer, according to Dawood, Jabbar, et al. (2018). The hot desert climate which affects the region causes the lowest temperatures to range from 7.9°C to 27.2°C, moreover, the temperatures could reach as high as 17.6°C to 45.6°C during the summer months of July and August, and occasionally passing the 50°C mark. In winter, the average temperature is 20°C, and due to the hot desert climate, that the governate experiences, the rate of rainfall is very low, which ranges from (7.78 to 148) mm annually from November to April, reflecting its arid desert nature (Dawood, Jabbar, et al., 2018). and Figure (1) illustrates the research area.

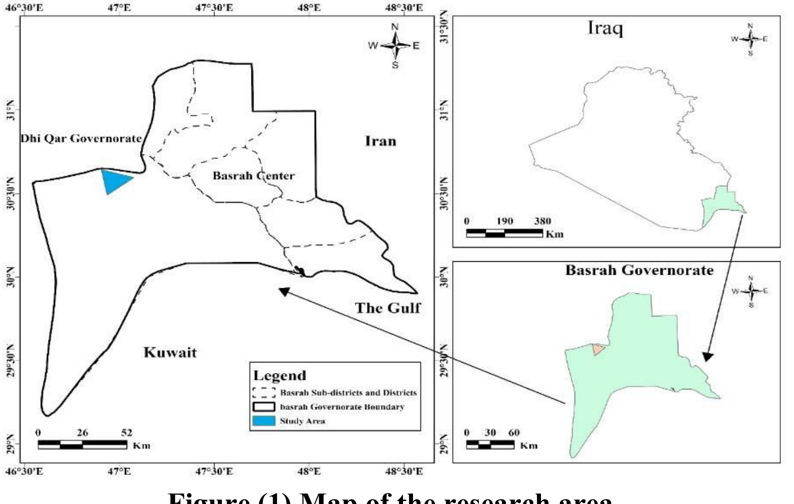

Figure (1) Map of the research area.

2-2 Data Sources and Preparation

To identify Groundwater Potential Zones (GWPZ), 7 positional layers (parameters) were prepared and integrated into the (ArcGIS Pro) environment. A satellite imagery was obtained with a spatial resolution of 30 meters from Landsat 8/OLI, which was then used to create a LULC map. A processing of the imagery followed, and then the (ISO Cluster) was used for unsupervised classification. The accuracy of the results was validated by comparison with Google Earth Pro 2024 imagery (U.S. Geological Survey, 2024). Average annual rainfall data for the period (2012-2024) were obtained from the TerraClimate dataset (Abatzoglou et al., 2018) and verified against the records of the Iraqi Meteorological Organization (IMOS, 2024). Next, the inverse distance weighting (IDW) method was used to spatially distribute the data. A 30-meter raster map of the groundwater depth was extracted from field well data measured in 2024, using the (IDW) spatial representation. Finally, the Digital Elevation Model (DEM) SRTM was used to derive the density of the drainage and slope layers, each with a resolution of 30 m (U.S. Geological Survey, 2014), where the slope values were extracted directly with the Slope tool in (ArcGIS Pro), a set of hydrological operations in the ArcGIS Pro environment were used to calculate the density of the drainage, these operations include Fill, Flow direction, Flow Accumulation and Stream Network in that order. Followed by the application of the Line Density tool in the unit (km/km^2). The coordinate system (WGS 1984 UTM Zone 38N) was also used as the seven positional layers got projected onto it, and their spatial resolution was rescaled to (30×30) m before applying the multi-criteria analysis, in order to achieve spatial homogeneity and geometric consistency among all the positional layers. Table (1) summarizes the details of the spatial datasets, their sources, and the processing methods that were adapted in this research.

Table 1. Information about the processing methods that were adopted in this study as well as the spatial data sources. (Abatzoglou et al., 2018; IMOS, 2024; U.S. Geological Survey, 2014, 2024)

Parameter	Data Source	Processing Methods
(LULC)	Landsat 8 OLI/TIRS (30m resolution) from USGS EarthExplorer (U.S. Geological Survey, 2024).	Preprocessing (Layer Stacking, Clipping), Unsupervised Classification(ISO Cluster), and Checking accuracy using Google Earth Google Earth Pro (2024).
Rainfall (Precipitation)	TerraClimate dataset (Abatzoglou et al., 2018) from Climate Engine (2012–2024), validated with Iraqi Meteorological	Employing the Inverse Distance Weighting (IDW) method to extract the average annual precipitation values and

	Organization and Seismology data.	spatial interpolation in ArcGIS Pro.
Slope Map	Digital Elevation Model (DEM) - SRTM with 30 m resolution from USGS EarthExplorer (U.S. Geological Survey, 2014).	Projecting data to the WGS 1984 UTM Zone 38N (metric system), then Slope extraction in Degrees by using the Slope tool in ArcGIS Pro.
Drainage Density	Digital Elevation Model (DEM) - SRTM with 30 m resolution from USGS EarthExplorer (U.S. Geological Survey, 2014).	Hydrological Processing in ArcGIS Pro (Fill, Flow Direction, Flow Accumulation), stream network extraction, then calculation of density using the Line Density tool (km/km²).
Depth to Groundwater	Field data from water wells within the study area for (2024) year.	Spatial mapping of wells coordinates and generating a raster, using spatial analyst tool, Inverse Distance Weighting (IDW) interpolation method.

2-3 Geospatial Thematic Layers

The Analytic Hierarchy Process (AHP) method, which is one of the widely applied multi-criteria decisions making (MCDM) methods, was employed to recognize the groundwater potential zone (GWPZ). This method was selected as a result of its advantages and widespread utilization in hydrological studies. Its most significant advantage is its high flexibility in dealing with the complexities of nature, as it allows for the integration of completely different layers into a single map. This enables the precise and rigorous analysis of multiple, overlapping factors (Abijith et al., 2020; Al-Abadi et al., 2016). Furthermore, this method is characterized by the ease with which results can be explained to decision-makers, and its findings closely match and align with actual field data from drilled wells. Also, the AHP method is ideal in areas lacking extensive data and large well counts (Chen et al., 2018; Ozegin & Ilugbo, 2024; Shinde et al., 2024). Additionally, this method combines human experience and digital maps, and provides a safety valve in the form of the consistency ratio (CR) (Al-Abadi & Al-Qurnawy, 2021; Al-Qurnawy et al., 2024; Ifediegwu, 2022). It integrates the (ArcGIS Pro) software environment and remote sensing (RS) techniques into a comprehensive methodology. The goal behind employing this methodology is to establish the effective parameters (thematic layers) weights in the groundwater recharge and measuring their significance, thereby reducing subjectivity and bias when assigning weights to each thematic layer. (Saaty, 1980; Machiwal et al., 2011; Arulbalaji et al., 2019; Pradhan et al., 2021)

Based on the methodology of hydrogeological principles and similar previous studies (Al-Qurnawy et al., 2024; Mukherjee et al., 2012; Das & Pardeshi, 2018; Ifediegwu, 2022), five thematic layers (parameters) were adopted to control groundwater occurrence and recharge, using (ArcGIS Pro) software. These thematic layers are:
1-Slope controls vertical infiltration rates compared to surface runoff, according to fundamental principles of hydrology (Todd & Mays, 2005).
2-The density of the drainage is in an inverse relationship with the permeability of the soil and therefore with the potential for groundwater.
3-The aquifers are recharged mainly through rainfall.
4- Infiltration, runoff, evaporation, and transpiration, which are all processes of hydrological cycles are influenced by LULC.
5- How close the wells are to the level of groundwater is signaled by the depth to groundwater level.

2-4 Analytic Hierarchy Process (AHP)

Thomas Saaty (1980) designed the Analytic Hierarchy Process (AHP) to assist multi-criteria decision making (MCDM) as a quasi-quantitative tool. In order to determine the relative weights of the elements, an analysis of the problem is conducted by the tool as it creates a hierarchy of the elements and the carries out a pairwise comparison between them. This methodology is used in groundwater mapping (Saravanan et al., 2021; Ifediegwu, 2022; Aykut, 2021; Pradhan et al., 2021).

2-4-1 Pairwise Comparison Matrix

The criteria are arranged in a square matrix from 1 to 9 (Saaty's Scale), and each pair of criteria is compared using Saaty's standardized scale (n × n). Saaty's scale that is used in pairwise comparisons is shown in Table (2). Each row represents one of the seven criteria and the same criteria are put in the columns. Saaty established a rule for filling in this table: if the symbol is (a_{ij}), then (a) represents the cell in the table or the element in the matrix, the letter (i) represents the criterion in the row, and the letter (j) represents the criterion in the column. The number placed in the cell ranges from (1 to 9) and expresses (how often the criterion in that specific row is more significant than the one in the column). The primary diagonal of the matrix, which in Saaty's scale takes the number (1), is represented by the symbol ($a_{ii} = 1$), as the criterion intersects itself. The ratio of the less significance criterion to the more important one when the comparison is inverted is represented by the symbol ($a_{ji} = 1/a_{ij}$) and is called the inverse property. (Saravanan et al., 2021; Ifediegwu, 2022; Aykut, 2021).

Table (2): Saaty's scale for pairwise comparison (saaty, 1980).

Intensity of Importance	Definition
1	Equal importance
2	Equal to moderate importance
3	Moderate importance
4	Moderate to strong importance
5	Strong importance
6	Strong to very strong importance
7	Very strong importance
8	Very to extremely strong importance
9	Extremely strong importance

Extraction of Normalized Weights: A pairwise comparison matrix was built based on expert opinions and a review of previous relevant scientific literature. Processing the columns is then done by dividing each value by the sum of its column. The geometric mean of each row is then calculated to obtain the final weight for each criterion (W_j - Normalized Weights). A sub-rank, designated as (r_i) or Class Rating, is assigned to evaluate the sub-classes of each criterion. These weights collectively reflect the contribution to groundwater potential. (Malczewski, 1999; Machiwal et al., 2011; Mukherjee et al., 2012; Pradhan et al., 2021; Ifediegwu, 2022; Aykut, 2021)

To ensure the highest mathematical accuracy, the weight vector law (Eigenvector - W_n) is derived based on the geometric mean, according to the following equation (1):

$$\boldsymbol{W_n} = \left(\frac{\boldsymbol{Gm}}{\sum_{i=1}^{n} \boldsymbol{Gm}}\right) \qquad (1)$$

Where: The criterion's final weight vector of the criterion is represented **by** W_n, and the geometric mean of row (i) in the comparison matrix is Gm.

2-4-2 Consistency Ratio Evaluation

To avoid any discrepancies in pairwise comparisons and to verify the mathematical logic derived from expert evaluations and previous studies, a calculation is then performed to obtain a coefficient called the Consistency Ratio

(CR) in order to establish the reliability of the extracted weights. This is the final step in the AHP approach, using the following equation (2) (Ying et al., 2007):

$$\mathbf{CR} = \frac{\mathbf{CI}}{\mathbf{RI}} \qquad \textbf{(2)}$$

Where: The Consistency Ratio is represented by CR is, and the Consistency Index is CI. While the Randomness Index (RI) is obtained from Saaty (1980) in a table based on the total number of criteria in this research, extracted from the approved standard tables as shown in Table (3) (Saaty, 1980).

Table (3) : Ratio Index (RI) values for n=1,2,3 … …,15 (Saaty, 1980).

N	1	2	3	4	5	6	7	8	9	10
RI	0.00	0.00	0.58	0.89	1.12	1.25	1.32	1.40	1.45	1.49

For statistical acceptance of weights, the CR value must not exceed 0.1, or CR ≤ 0.1. If this value is exceeded, the paired evaluations must be reviewed and adjusted until the condition is met.

The CR value is established after using the equation (3) shown below to calculate the Consistency Index (CR)

$$\boldsymbol{CI} = \frac{\boldsymbol{\lambda_{max} - n}}{\boldsymbol{n-1}} \qquad \textbf{(3)}$$

Where: The main eigenvalue of the matrix is λ_{max}, the overall number of criteria (thematic layers employed in this study) is (n), and determining the principal eigenvalue (λ_{max}) of the after calculating it using the following equation (4):

$$\boldsymbol{\lambda_{max}} = \frac{\mathbf{1}}{\boldsymbol{n}} \sum_{\boldsymbol{i=1}}^{\boldsymbol{n}} \frac{(\boldsymbol{A_w})_{\boldsymbol{i}}}{\boldsymbol{w_i}} \qquad \textbf{(4)}$$

Where: The weighted sum vector is represented by $(A_w)_i$ and is calculated after multiplying the final weights vector by the matrix of pairwise comparisons**.**

2-5. Groundwater Potential Index and Spatial Overlay (GWPI)

After obtaining the final approved weights for all criteria, the analysis is executed within the Geographic Information Systems environment (ArcGIS pro). Using a raster calculator or a weighted overlay tool, all layers are combined, and the weighted overlay equation is applied to produce a groundwater potential zone index (GWPZI) using the following equation (5):

$$\boldsymbol{GWPZI} = \sum_{\boldsymbol{i=1}}^{\boldsymbol{n}} (\boldsymbol{W_j} \times \boldsymbol{r_i}) \qquad \textbf{(5)}$$

Where the symbol (GWPZI) represents the groundwater potential zone index. This equation can be broken down to rank the seven parameters (positional layers) as follows:

$$\boldsymbol{GWPZI} = (\boldsymbol{W_{WD}} \times \boldsymbol{r_{WD}}) + (\boldsymbol{W_{SL}} \times \boldsymbol{r_{SL}}) + (\boldsymbol{W_{R}} \times \boldsymbol{r_{R}}) + (\boldsymbol{W_{LULC}} \times \boldsymbol{r_{LULC}}) + (\boldsymbol{W_{DD}} \times \boldsymbol{r_{DD}})$$

This equation produces a raster map containing continuous values for the Groundwater Potential Index (GWPZ), reflecting the relative potential of each pixel in the area of the research. With the ranges taken into mind, the map is then arranged, each representing a degree and level of groundwater potential for specific areas within the study region (Saravanan et al., 2021; Mukherjee et al., 2012; Arulbalaji et al., 2019; Das & Pardeshi, 2018). The methods employed in this study as well as the data are illustrated in Figure (2) in the form of a Flow chart.

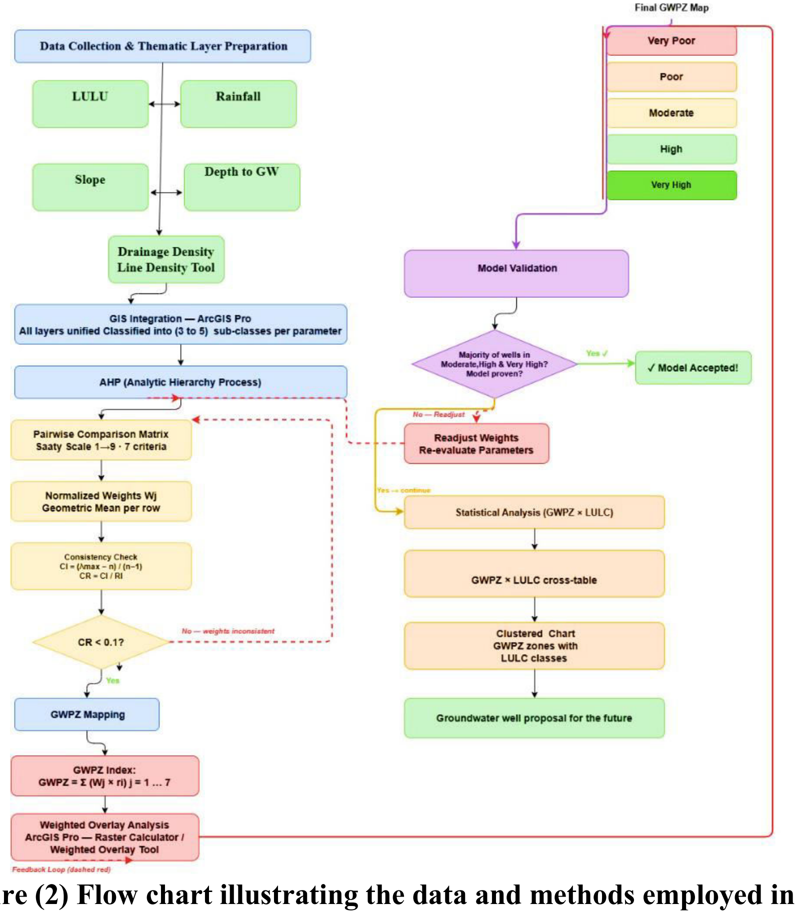

Figure (2) Flow chart illustrating the data and methods employed in this study.

Results and Discussion

3-1 Analytic Hierarchy Process Analysis (AHP): Table (4) shows the pairwise comparison matrix which was constructed for the study area by utilizing the Saaty (1980) scale which is presented in Table (2) with the five main thematic layers: depth to groundwater (WD), LULC, slope (SL), drainage density (DD), and rainfall (R). The comparison was conducted using the same scale, and the hydrogeological significance in controlling groundwater recharge and storage in the desert environment for the area of the study played a role in determining the relative significance of each criterion. The groundwater depth criterion was given the highest importance among the study criteria after the geology and soil type criteria were disregarded and considered homogeneous and fixed factors, despite their hydrogeological importance in groundwater recharge. This is because each criterion has only one type. The fundamental principle to be maintained is that a criterion with only one type does not provide any spatial variation (there is complete homogeneity between these two criteria, as the entire study area covers a single geological unit and a single soil type, which contradicts the principles of Multi-Criteria Spatial Analysis (GIS-MCDA)). The main purpose of integrating maps into the Weighted Overlay tool in GIS is to find spatial variation and differences. However, with the geology and soil type criteria, it is not possible to rank good and bad areas under a single criterion due to the lack of diversity in categories, which consumes part of the total weight. It would be more appropriate to distribute this weight among other criteria that have real variation to illustrate differences more accurately. This is what led to considering the geology and soil criteria as conditions. A fundamental boundary characterizes the general characteristics of the basin, and it was excluded from the pairwise comparison matrix in the (AHP) method, so that the analysis was limited to the five criteria with effective spatial variance, which raises the accuracy of the statistical and spatial outputs of the model. Hence, the groundwater depth criterion was preferred, as shallow water depths indicate the presence of saturated zones and high recharge of the aquifer, a result that aligns with the findings of a number of other studies (Pradhan et al., 2021) and (Saravanan et al. (2021). As for the second parameter, the LULC came in second place due to its important role in controlling surface water infiltration and generating surface runoff and evaporation. In addition, the study area has witnessed significant agricultural development in the last twenty years, which highlights the factor of human intervention through agriculture and its substantial impact on the potential zones for groundwater in the area which the study was conducted on. This principle is supported by many studies (Leduc et al., 2001; Abijith et al., 2020). The slope criterion ranked third, as this criterion effectively influences the balance between surface runoff and infiltration. Gentle slopes retain water for longer periods and enhance groundwater recharge (Saravanan et al., 2021). Next came the drainage density criterion, which reflects its inverse relationship with permeability (Saranya and Saravanan, 2020). The rainfall criterion ranked last because rainfall is very low and limited in scope in the study area, thus restricting its ability to stand out as a spatial indicator (Saaty, 1980; Ghorbani et al., 2016; Malczewski, 1999).

The consistency ratio (CR) values for the five parameters ranged from 0.015 for the drainage density criterion to 0.032 for the depth to groundwater criterion. The average consistency for the study criteria was 0.022, which is significantly lower than the 0.1 value established by Saaty (1980). This finding completely aligns with the judgments of the pairwise comparison matrix, and that the inferred weights are reliable for mapping groundwater potential zones. Verifying internal consistency is a crucial step in validating studies based on the Analysis Hierarchy Process (AHP), as it quantitatively measures the degree of logical coherence in the expert judgments of the studies upon which the analysis was based. (Saaty, 1980; Saravanan et al., 2021; Pradhan et al., 2021; Aykut, 2021; Ifediegwu, 2022). Table (5) shows how to extract the value of (CR).

Table (4) : The pairwise comparison matrix . (WD= depth to groundwater, LULC= Land use and Land cover, DD= Drainage Density, SL= Slope, GM= Geometric mean, R= Rainfall, w_i = Normalized weight).

parameter	**WD**	**LULC**	**SL**	**DD**	**R**	**GM**	**W_i**
WD	1	3	4	5	6	3.245342	0.487504
LULC	1/3	1	2	3	4	1.515717	0.227685
SL	1/4	1/2	1	2	3	0.944088	0.141817
DD	1/5	1/3	1/2	1	2	0.581811	0.087397
R	1/6	1/4	1/3	1/2	1	0.370107	0.055596
SUM	1.95	5.08333333	7.833333	11.5	16	6.657064	1

Table (5): The greatest eigenvalue of pair wise comparison decision matrix (λmax), consistency index (CI), random consistency index (RI) and consistency ratio (CR) for the parameters.

Parameter	**W_i**	**$(Aw)_i$**	**λmax**	**CI**	**CR**
WD	0.487504	2.508394	5.145386	0.036347	0.032452
LULC	0.227685	1.158399	5.087715	0.021929	0.019579
SL	0.141817	0.719119	5.070742	0.017686	0.015791
DD	0.087397	0.442894	5.067586	0.016897	0.015086
R	0.055596	0.284739	5.121565	0.030391	0.027135

Sum	**1.000**	1	5.098599	**Average**	0.022

3-2. Characteristics of Thematic Layers

Table (6) shows the process of combining the final weights (Wi) that were extracted through employing the (AHP) method from the pairwise comparison matrix in Table (4). It also shows the division of each layer into subcategories ranked based on its expected contribution to groundwater recharge potential. A sub-class normalized weight was calculated by dividing the category rank by the sum of the ranks for the same criterion, and finding the area and percentage of each of the five criterion categories used within the (ArcGIS pro) program for the study area.

Table 6: Normalized weights, ranks, and areas for the thematic layers and their subclasses

Thematic Layer (Parameter)	Normalized Weight (w_i) for Thematic Layer	Subclasses	Rank	Normalized Weight (w_i) for Subclasses	Subclass Area (km²)	Subclass Area (%)
Depth to Groundwater (WD)	0.4875	(11.67-13.8) m	5	0.3333	44.45	33.51%
		(13.8-15.8) m	4	0.2667	36.61	27.60%
		(15.8-18.0) m	3	0.2	18.78	14.16%
		(18.0-19.75) m	2	0.1333	23.97	18.06%
		(19.75-21.74) m	1	0.0667	8.85	6.67%
Land Use/Land Cover (LULC)	0.2277	Agriculture	4	0.4	46.13	34.77%
		Grasses	3	0.3	62.33	46.98%
		Barren Land / Wasteland	2	0.2	22.35	16.85%
		Urban Area	1	0.1	1.85	1.39%
Slope (SL)	0.1418	(0-1.5)°	5	0.3333	82.35	62.08%
		(1.5-3.0)°	4	0.2667	44.8	33.77%
		(3.0-5.0)°	3	0.2	5.38	4.05%
		(5.0-6.5)°	2	0.1333	0.12	0.10%
		(6.5-8.148)°	1	0.0667	0.01	0.0001%

Drainage Density (DD)	0.0874	(0-0.44) km/km²	5	0.3333	20.27	15.28%
		(0.44-0.88) km/km²	4	0.2667	32.47	24.47%
		(0.88-1.30) km/km²	3	0.2	36.37	27.42%
		(1.30-1.77) km/km²	2	0.1333	28.36	21.38%
		(1.77-2.90) km/km²	1	0.0667	15.19	11.45%
Rainfall (R)	0.0556	(90-91) mm	3	0.5	15.2	11.46%
		(87-90) mm	2	0.3333	100.29	75.60%
		(86-87) mm	1	0.1667	17.17	12.94%

In this study, the weights and ranks of the subject layers and their categories were not assigned randomly, but were based on basic hydrogeological principles. The general rule states that categories that promote infiltration rates and limit surface runoff are given higher weights and ranks, given their direct contribution to groundwater recharge.

Based on statistical analysis that was obtained after employing the Analytic Hierarchy Process (AHP) algorithm, and supported with expert opinions and the methodology of previous studies in arid and semi-arid environments, the five criteria were classified and evaluated in line with the spatial and topographical characteristics of the study area, as follows:(Saravanan et al., 2021; Ifediegwu, 2022; Aykut, 2021; Pradhan et al., 2021; Mukherjee & Singh, 2020; Al-Ruzouq et al., 2019; Abdelkareem et al., 2022)

3-2-1 Depth to Groundwater (WD): After the geological and soil type criteria were disregarded for the aforementioned reasons, the depth to groundwater criterion emerged as a direct hydrogeological indicator of the proximity of the saturated zone to the Earth's surface, as it reflects the cumulative effect of withdrawal and recharge processes. Classification and ranking are based on the principle that water infiltrating from the Earth's surface, whether from rain or irrigation, will reach the shallow aquifer more quickly and with less loss in the non-infiltrating zone, making its exploitation easier and less costly. This aligns with the principle that a lower water depth indicates increased storage capacity and improved recharge efficiency, a finding consistent with numerous previous studies. (Arnous et al., 2020; Pradhan et al., 2021; Machiwal et al., 2011; Arulbalaji et al., 2019; Etikala et al., 2019). This principle was applied to the area of the research, with the criterion of groundwater depth being assigned a standardized weight. Its value is 0.4875. This criterion was classified into 5 classifications using the Manual Interval method. The shallow depths (11.67 - 13.8) meters were ranked highest (Rank=5), encompassing an area of 44.45 km², accounting for (33.51%) of the region. In contrast, the deeper areas (19.75 - 21.74) meters were ranked lowest (Rank=1), encompassing an area of 8.85 km², accounting for (6.67%). (Arnous et al., 2020; Machiwal et al., 2011; Pradhan et al., 2021). Figure (3) shows the map for the depth to groundwater in the area of the research.

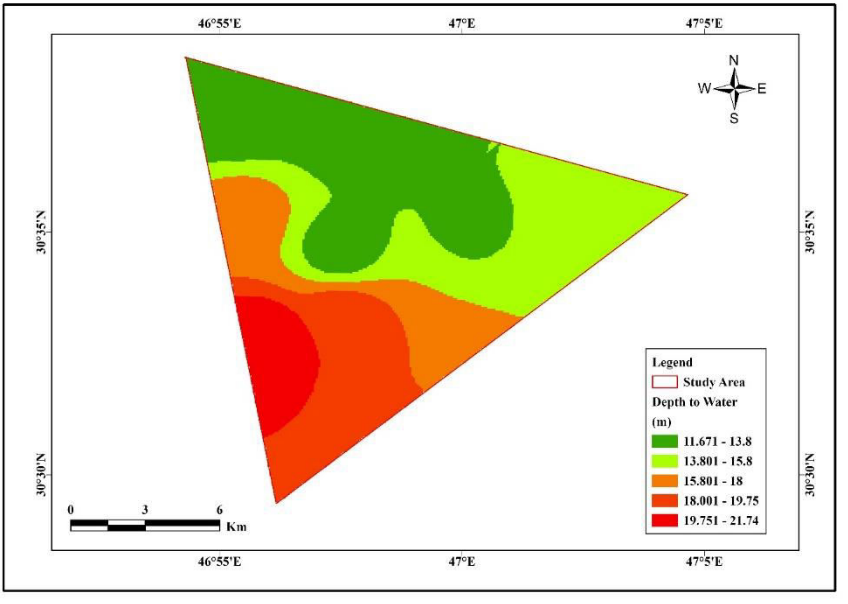

Figure (3) The depth to groundwater map in the area of the research.

3-2-2-Land Use and Land Cover (LULC): Given how crucial LULC is as a direct factor affecting surface runoff and infiltration, this criterion with a standard weight of 0.2277 was ranked second. The study area included 4 classifications using the Unique Values method, which is most suitable for qualitative data. The agriculture category had the highest rank (Rank = 4) and covered an area of the study area estimated at 46.13 km^2, representing 34.77%. The second highest rank category was grasses (Rank = 3), covering an area of 62.33 km² of the study area, representing 46.98%. This is justified by the fact that agricultural activities and grazing increase surface roughness, hindering surface runoff and promoting infiltration. Furthermore, continuous tillage and irrigation can sometimes create backflow into the aquifer, acting as a secondary source of groundwater recharge. In contrast, wasteland ranked third (Rank = 2), covering an area of 22.35 km², or 16.85%, due to its compacted soil. Finally, urban areas ranked last (Rank = 1) because their impermeable surfaces completely prevent infiltration and increase surface runoff, covering an area of 1.85

km², or 1.39%. This assessment aligns with the findings of numerous studies worldwide that have evaluated this criterion for groundwater recharge.

(Saravanan et al., 2021; Leduc et al., 2001; Abijith et al., 2020; Mukherjee & Singh, 2020; Pinto et al., 2017). The LULC map of the research area is shown in Figure (4).

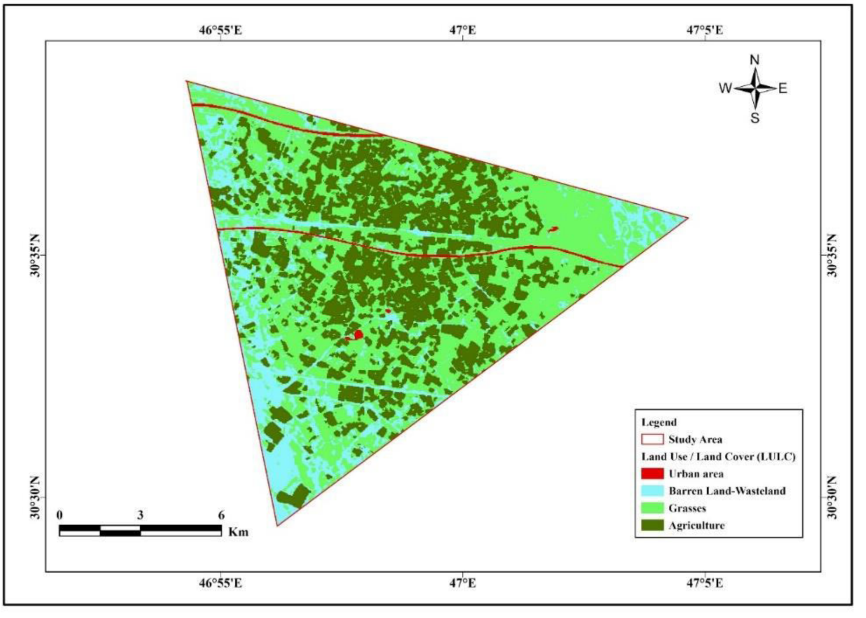

Figure (4) LULC map of the area of the research.

3-2-3 Slope: The dynamics and speed of surface runoff are affected by the slope factor, which also facilitates the influence on the time period available to infiltrate the subsurface by the water. It has been given a standard weight of 0.1418. According to the inverse relationship between the degree of slope and the opportunity for recharge, and since flat terrain increases the time of residence of water and allows it to stagnate, this reduces the speed of surface runoff and provides ideal conditions for vertical penetration towards the aquifer. This criterion was classified into 5 categories using the Manual Interval method. The semi-flat areas (0.0–1.50) received the highest rating, rank 5, covering the vast majority of the area at 82.35 km², representing 62.08%. Conversely, the steep areas (6.50–8.148) received the lowest rating, rank 1, as they accelerate runoff and prevent the land from absorbing water. Only a modest part of the research area was covered by these areas, approximately 0.01 km². Many previous studies have adopted this scientific interpretation for classifying this parameter. (Aykut, 2021; Ifediegwu, 2022; Machiwal et al., 2011; Pinto et al., 2017)**.** The slope map for the area of study is shown in Figure (5).

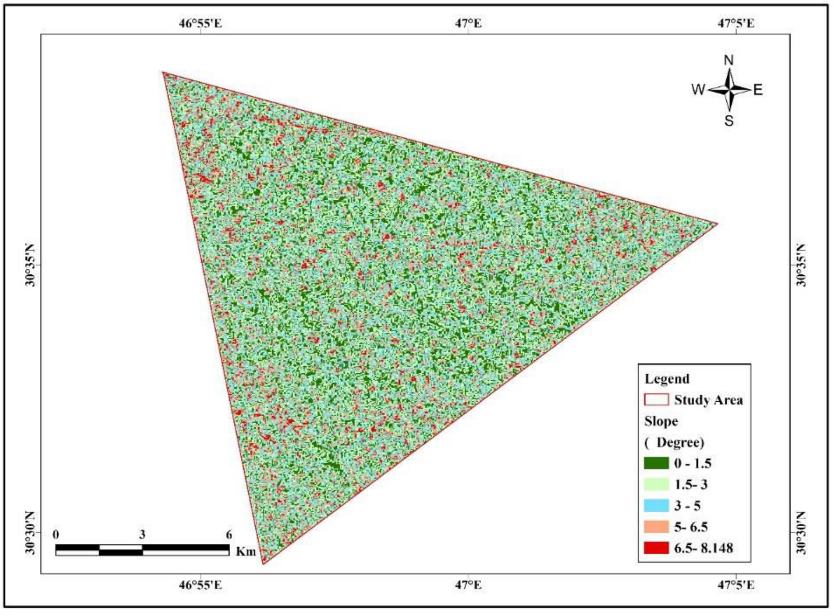

Figure (5) The slope map of the area of study.

3-2-4 Drainage Density: The fundamental idea behind this classification method, which has a standard weight of 0.0874, is that a lower density of drainage is an indication that highly permeable materials exist in the surface, allowing rainwater to seep directly into the ground without forming dense surface runoff networks. Conversely, areas that are characterized with high density of drainage suggest the presence of impermeable rock formations or low-permeability soils that force water to run off the surface quickly and limit deep infiltration (Todd & Mays, 2005), thus leading to branching and condensation of watercourses. This methodological consistency is supported by studies confirming that a low drainage density is a strong indicator of a high rate of groundwater recharge (Greenbaum, 1992; Yeh et al., 2016; Zhu & Abdelkareem, 2021; Saranya and Saravanan, 2020)

This parameter was classified into 5 categories using the Natural Break (Jenks) method. The lowest drainage density category (0-0.44) km/km² received the highest rank (rank 5), covering an area of 20.27 km², representing 15.28%. The highest drainage density category (1.77-2.9) km/km² received the lowest rank (rank 1), covering an area of 15.19 km², representing 11.45%. The drainage density map for the research area is illustrated in Figure (6).

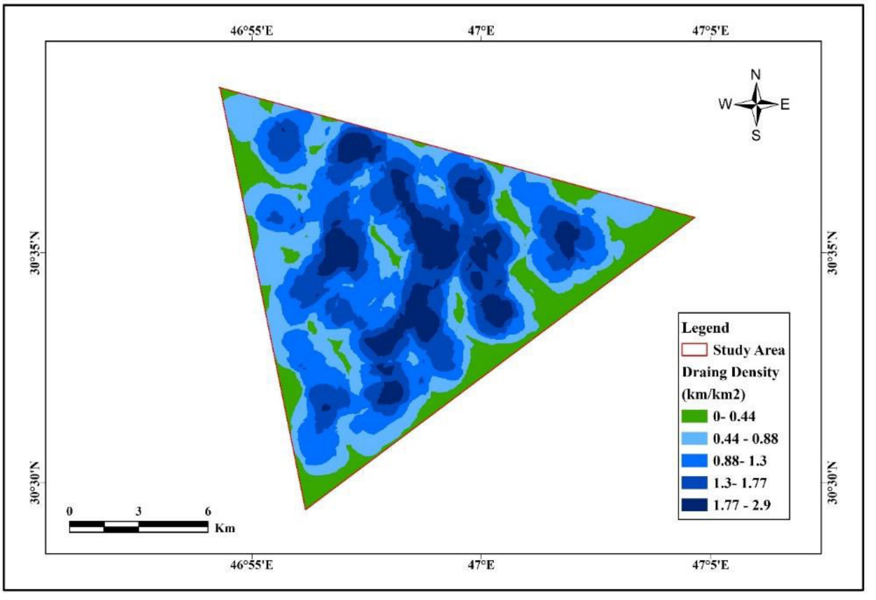

Figure (6) The drainage density map for the area of the research.

3.2.7 Rainfall: Given the low rainfall and the narrow spatial variation within the study area, which ranged only between (86 - 91) mm, this parameter was assigned a low standard weight of 0.0556. The classification method was based on the scientific principle that any increase in rainfall, even a small one, supports the aquifer as thee increase causes a greater amount of water available for effective infiltration into the aquifer. This is directly proportional to the groundwater's protection, a principle supported by previous studies. (Adiat et al., 2012; Aykut, 2021; Saravanan et al., 2021).

This parameter was classified into three categories using the Manual Interval method. The highest rainfall amounts (90-91 mm) received the highest rating, ranking 3 (rank = 3), and covered an area of 15.2 km², representing 11.46%. The lowest rainfall amounts (86-87 mm) were rated as rank 1, covering an area of 17.17 km² and representing 12.94% of the whole area. The rainfall map for the area of the research is shown in Figure (7).

3-3 Spatial Distribution of Groundwater Potential Zones (GWPZ)

After calculating the relative weights of each positional layer (parameter) of the study criteria using the Analysis Hierarchy Matrix (AHP) and then integrating them into ArcGIS Pro, the Raster Calculator tool via the weighted linear combination (WLC) equation was employed in calculating the final Groundwater

Potential Zones (GWPZ) index. This allowed for precise integration of the floating-point weights, resulting in a high-resolution groundwater potential map, which appeared as follows:

$$GWPZ \quad Index = \sum[w_i \times r_i]$$
$$GWPZ = (0.4875 \ \times \mathrm{WD_{Rank}}) + (0.2277 \ \times \mathrm{LULC_{Rank}}) + (0.1418 \ \times \mathrm{SL_{Rank}}) + (0.0874 \ \times \mathrm{DD_{Rank}}) + (0.0556 \ \times \mathrm{R_{Rank}})$$

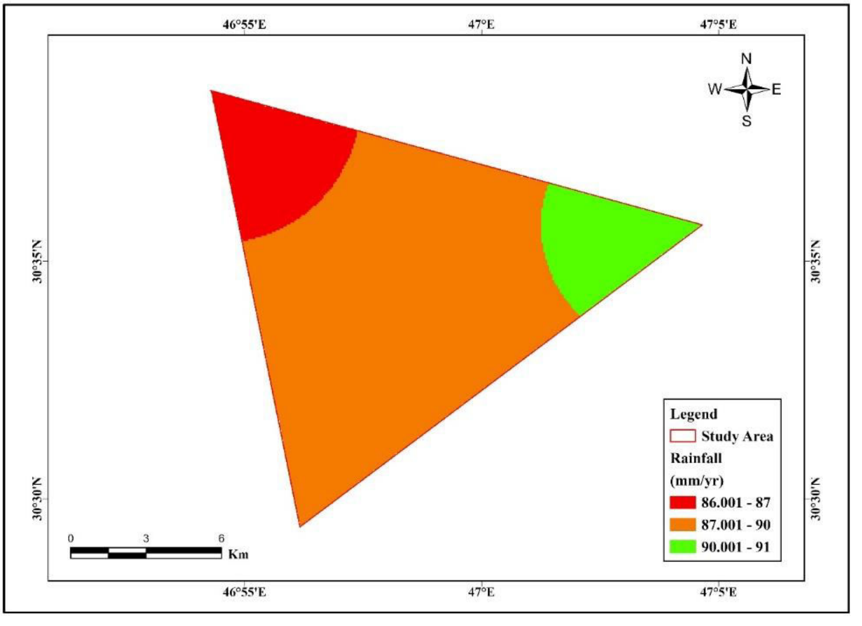

Figure (7) The rainfall map of the area of the research.

The Natural Break (Jenks) method was adopted in this study to create five categories and classify the potential zones for groundwater in them. This method proved most suitable for the study area, minimizing intra-category variability and maximizing inter-category differences, thus generating an accurate representation of spatial variation in groundwater potential. The five categories were: very low potential (1.568–2.449), low potential (2.45–2.997), moderate potential (2.998–3.557), high potential (3.558–4.034), and very high potential (4.035–4.605). The high potential category covered approximately one-third of the total area (30.61%), meanwhile, zones with very high and moderate potential covered a substantial area with 26.56% and 17.23% respectively. while the low and very low groundwater potential categories covered only 17.43% and 8.17% respectively. Thus, great portion of the research area equal to 74.4% is considered to possess moderate, high, and very high potential for groundwater, the main concentration of in the research area was from the northern side to the central part of the southern side. The remaining left side of the southern part of the research area saw the existence of the low and very low potential groundwater categories. A map of the potential zones for groundwater in the research area is shown is Figure (8).

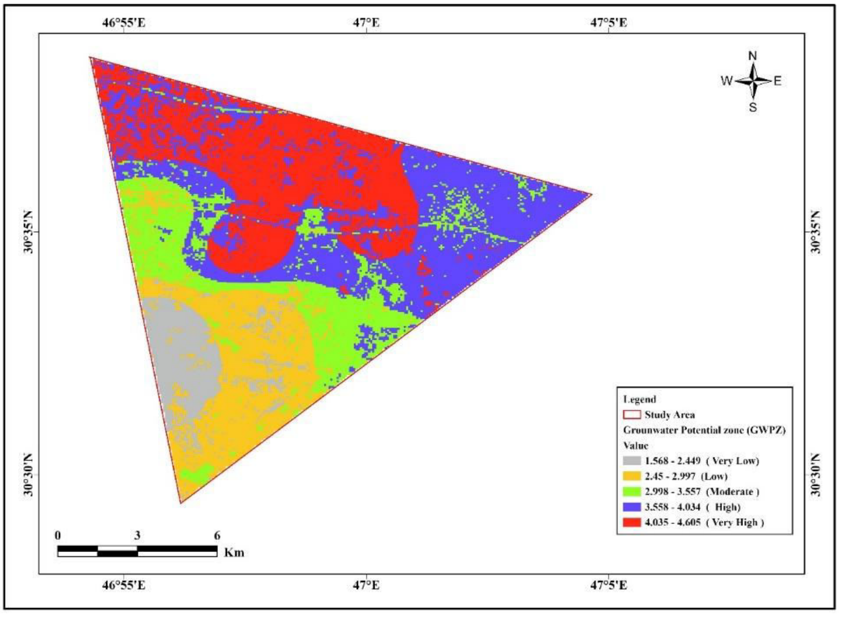

Figure (8) A map of the potential zones for groundwater in the research area.

3-4 Model Validation

Five Groundwater Potential Zones (GWPZ) categories were matched with the locations of ten wells in the research area to evaluate the predicted model, this showed that 6 wells correspond to zones with high to very high potential, 2 wells correspond to zones with medium potential, and 2 wells correspond to zones with low and very low potential. Therefore, a substantial percentage of the wells in the research area equal to 80% are located within zones with very high, high, and medium potential, demonstrating the accuracy of the study model. Several studies have supported this approach to model validation (Zhu & Abdelkareem, 2021; Arnous et al., 2020). Figure (9) illustrates the wells locations in the research area.

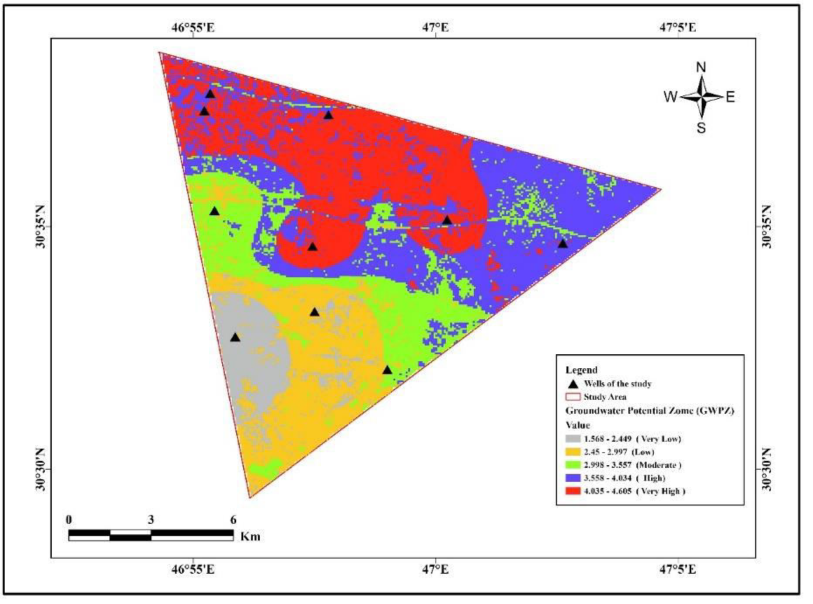

Figure (9) The locations of the wells in the research area.

3-5 Quantitative and Spatial Distribution between (GWPZ) Zones and (LULC) Classes:

A post-classification spatial tabular cross-distribution was performed to quantify the cross-distribution between predicted groundwater potential zones and current land use patterns using the ArcGIS Pro environment for the study area. Table (7) illustrates the quantitative cross-distribution between land uses and vegetation cover with groundwater potential zones by presenting the spatial distribution of the four LULC categories in the research area (Urban area, barren land, Grasses, and Agriculture) within each of the five groundwater potential categories (GWPZ): very low, low, moderate, high, and very high.

Table (7) Distribution of (LULC) categories within each (GWPZ) category

Parameter	Urban (Km^2)	Wasteland (Km^2)	Grasses (Km^2)	Agriculture (Km^2)	Sum (Km^2)
very low	1.149	73.337	44.737	13.438	132.662
low	1.965	35.642	61.943	33.112	132.662
moderate	4.467	20.022	66.358	41.814	132.662
high	1.824	17.750	74.631	38.457	132.662

very high	0.124	3.446	51.064	78.028	132.662

Figure (10) illustrates the ratio of LULC classifications within the groundwater potential categories (GWPZ). The results showed a direct relationship between agriculture and groundwater potential, with agricultural land increasing significantly from 10.13% in very low potential areas to 58.82% in very high potential areas. This clearly indicates that agricultural activity is concentrated in areas with high groundwater potential. The study showed that agriculture and grassland combined are present at their highest percentage in both very high and high groundwater potential areas, at (97.31%) and (85.25%), respectively. Conversely, the study revealed an inverse relationship between groundwater potential and the percentage of barren land, decreasing from 55.28% in very low potential areas to 2.6% in very high potential areas. This indicates that agricultural land and grasses displace barren land as groundwater potential increases. As for urban areas, the results indicated that they peak in regions with a medium potential of 3.37% and recedes in areas with a very high potential, which indicates that urban areas are located further from shallow groundwater zones.

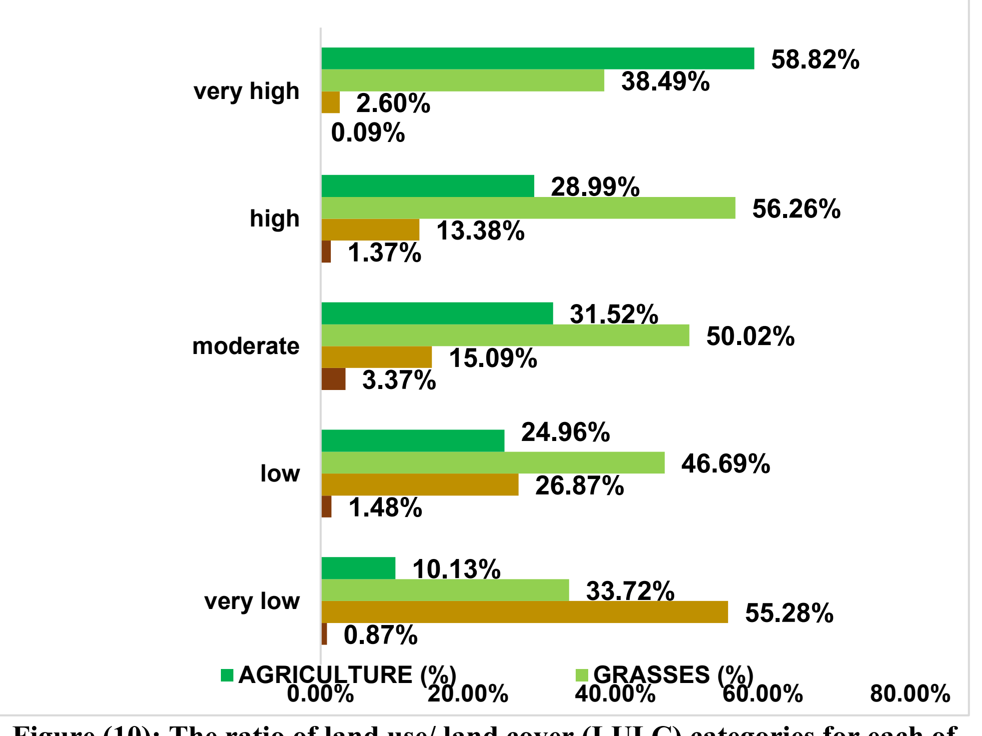

Figure (10): The ratio of land use/ land cover (LULC) categories for each of The Groundwater Potential Categories (GWPZ).

3-6 Proposed Sites for Future Groundwater Wells:

According to the final potential zones for groundwater map results, the research suggests identifying sites for drilling new future wells. (26) future well sites have been proposed, concentrated exclusively within areas with high and very high potential, as Figure (11) illustrates. This proposed map aims to provide a guiding tool for decision-makers and planners to ensure the most successful and sustainable spatial management of the water resource. To ensure the sustainability of this aquifer, the study recommends the necessity of establishing a comprehensive monitoring system that includes the construction of dedicated monitoring wells to take periodic measurements of water levels in areas with the very high and high potential.

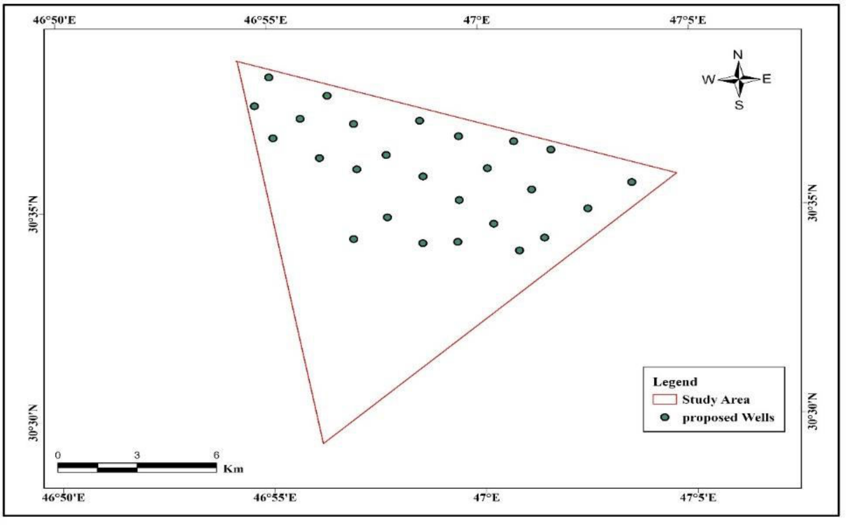

Figure (11) Proposed Sites for Future Groundwater Wells

Conclusions:

The study demonstrated the effectiveness of integrating Analysis Hierarchy Technique (AHP) and the (ArcGIS PRO) software environment in identifying groundwater potential zones GWPZ and in finding the quantitative intersection between GWPZ and LULC, through thematic layers consistent with the nature of the region and its desert environment, where rainfall was the least important parameter due to scarcity and narrow spatial variation. Zones with high potential alone represented (30.61%) of the research area, while very high and medium potential zones comprised 26.56% and 17.23%, respectively. Meanwhile, zones with very low and low potential covered 17.43% and 8.17%, respectively, of the research area. The northern to the central and southern parts of the research area saw a concentration of zones with medium, high, and very high potential, while zones with low and very low potential for groundwater were concentrated on the remaining left side of southern portion of the research area. The quantitative correlation between GWPZ and LULC demonstrated a correlation between human activities and hydrogeological conditions. Agricultural areas and grasses were concentrated in the very high potential zones, while urban areas were located further away from these zones, concentrating more heavily in the medium potential zones. Barren lands, however, exhibited an inverse relationship with groundwater potential zones. In addition, the field matching between the producing wells and the expected model constituted a supporting strength factor for the accuracy of the model. Hence, the study was able to create a scientific model applicable in areas similar to the study conditions, which contributes to directing drilling operations towards the most sustainable and economically viable areas, by proposing the establishment of 26 wells in very high and high potential areas, which helps decision-makers in better management of the groundwater stock in this area, provided that this is accompanied by the work of a comprehensive monitoring system through the establishment of monitoring wells and taking periodic measurements of water levels in the very high and high potential areas.

References

Abatzoglou, J. T., Dobrowski, S. Z., Parks, S. A., & Hegewisch, K. C. (2018). TerraClimate, a high-resolution global dataset of monthly climate and climatic water balance from 1958–2015. *Scientific Data*, *5*(1), 170191. https://doi.org/10.1038/sdata.2017.191

Abdelkareem, M., Al-Arifi, N., Abdalla, F., Mansour, A., & El-Baz, F. (2022). Fusion of remote sensing data using GIS-based AHP-weighted overlay techniques for groundwater sustainability in arid regions. *Sustainability*, *14*(13), 7871. https://doi.org/10.3390/su14137871

Abdulameer, A., Thabit, J. M., AL-Menshed, F. H., & Merkel, B. (2018). Investigation of seawater intrusion in the Dibdibba Aquifer using 2D resistivity imaging in the area between Al-Zubair and Umm Qasr, southern Iraq. *Environmental Earth Sciences*, *77*(17), 619. https://doi.org/10.1007/s12665-018-7798-3

Abdullah, P. D. S. S. (2024). Temporal variation of salinity in the Middle Shatt al-Arab River, southern Iraq. *Basra Studies Journal*, *1*(55), 143–164.

Abijith, D., Saravanan, S., Singh, L., Jennifer, J. J., Saranya, T., & Parthasarathy, K. S. S. (2020). GIS-based multi-criteria analysis for identification of potential groundwater recharge zones—A case study from Ponnaniyaru watershed, Tamil Nadu, India. *HydroResearch*, *3*, 1–14. https://doi.org/10.1016/j.hydres.2020.02.002

Adiat, K. A. N., Nawawi, M. N. M., & Abdullah, K. (2012). Assessing the accuracy of GIS-based elementary multi criteria decision analysis as a spatial prediction tool – A case of predicting potential zones of sustainable groundwater resources. *Journal of Hydrology*, *440–441*, 75–89. https://doi.org/10.1016/j.jhydrol.2012.03.028

Ahmed, A. R., & Al-Zewar, J. M. (2020). Socio-economic impact of the saltwater intrusion in the Shatt al-Arab River on fish farmers in Al-Mashab marshes, Southern Iraq.

Al Aboodi, A. H., & Munshid, H. F. (2017). A two-dimensional numerical model of groundwater flow in Safwan AlZubair area, South of Iraq. *University of Thi-Qar Journal for Engineering Sciences*, *8*(3), 40–54. https://doi.org/10.31663/utjes.v8i3.96

Al-Abadi, A. M. A., & Al-Qurnawy, L. S. (2021). Control the effect of groundwater rising using GIS and multi-criteria decision making techniques in Zubair, south of Iraq. *The Iraqi Geological Journal*, 93–104. https://doi.org/10.46717/igj.54.1D.8Ms-2021-04-28

Al-Abadi, A. M., Al-Temmeme, A. A., & Al-Ghanimy, M. A. (2016). A GIS-based combining of frequency ratio and index of entropy approaches for mapping groundwater availability zones at Badra–Al Al-Gharbi–Teeb areas, Iraq. *Sustainable Water Resources Management*, *2*(3), 265–283. https://doi.org/10.1007/s40899-016-0056-5

Al-Ansari, N. (2021). Topography, climate, and water resources of Iraq. *Journal of Earth Sciences and Geotechnical Engineering*, 1–34. https://doi.org/10.47260/jesge/1122

Al-Asadi, S. A. R., & Alhello, A. A. (2019). *General assessment of Shatt Al-Arab River, Iraq*. https://faculty.uobasrah.edu.iq/uploads/publications/1631354254.pdf

Albhadili, S., Almallah, I., & Almulla, S. (2023). Mapping ground water potential recharge zones of Wadi Al-Batin alluvial fan, using remote sensing and GIS techniques, southwestern Iraq. *Iraqi Bulletin of Geology and Mining*, *19*(1a), 99–115. https://doi.org/10.59150/ibgm1901a07

Al-Jiburi, H. K., & Al-Basrawi, N. H. (2011). Hydrogeology of the Mesopotamia plain. *Iraqi Bulletin of Geology and Mining*, (4), 83–103.

Al-Kaaby, L. F., & Albadran, B. N. (2020). Minerals and sedimentary characteristics of Quaternary sediments of different regions in southern Iraq. *The Iraqi Geological Journal*, 68–89. https://doi.org/10.46717/igj.53.1a.R5.2020.01.27

Al-Mahmood, H. K., & Mahmood, A. B. (2019). Effect of Karun River on the salinity status in the Shatt Al-Arab River, Basrah—Iraq. *Mesopotamian Journal of Marine Sciences*, *34*(1), 13–26. https://doi.org/10.58629/mjms.v34i1.42

Al-Mallah, I. A., Al-Qurnawi, W. S., Ghalib, H. B., Al Hawash, A. B., & Abdulameer, M. H. (2022). Evaluation of groundwater quality in the Dibdibba aquifer using hydrogeochemical and isotope techniques (Basrah Province, Iraq). *Acta Geochimica*, *41*(5), 823–838. https://doi.org/10.1007/s11631-022-00549-8

Almuktar, S., Hamdan, A. N. A., & Scholz, M. (2020). Assessment of the effluents of Basra city main water treatment plants for drinking and irrigation purposes. *Water*, *12*(12), 3334. https://doi.org/10.3390/w12123334

Alqurnawy, L. S., Almallah, I. A., & Alrubaye, A. (2022). Groundwater vulnerability analysis via GALDIT-GIS method to seawater intrusion, south of Iraq. *The Iraqi Geological Journal*, 146–161. https://doi.org/10.46717/igj.55.1E.12Ms-2022-05-28

Al-Qurnawy, L., Almallah, I., & Alrubaye, A. (2024). Hydrochemical characteristics and spatial variability in coastal aquifers southern Iraq utilizing a GIS technique. *The Iraqi Geological Journal*, 264–276. https://doi.org/10.46717/igj.57.2C.18ms-2024-9-26

Al-Ruzouq, R., Shanableh, A., Merabtene, T., Siddique, M., Khalil, M. A., Idris, A., & Almulla, E. (2019). Potential groundwater zone mapping based on geo-hydrological considerations and multi-criteria spatial analysis: North UAE. *CATENA*, *173*, 511–524. https://doi.org/10.1016/j.catena.2018.10.037

Al Saad, Z. A. A., & Hamdan, A. N. A. (2020). Evaluation of water treatment plants quality in Basrah Province, by factor and cluster analysis. *Journal of Water and Land Development*, 10–19. https://doi.org/10.24425/jwld.2020.134097

Al-Sudani, H. I. Z. (2019). Groundwater system of Dibdibba sandstone aquifer in south of Iraq. *Applied Water Science*, *9*(4), 72. https://doi.org/10.1007/s13201-019-0952-6

Arnous, M. O., El-Rayes, A. E., Geriesh, M. H., Ghodeif, K. O., & Al-Oshari, F. A. (2020). Groundwater potentiality mapping of tertiary volcanic aquifer in IBB basin, Yemen by using remote sensing and GIS tools. *Journal of Coastal Conservation*, *24*(3), 27. https://doi.org/10.1007/s11852-020-00744-w

Arulbalaji, P., Padmalal, D., & Sreelash, K. (2019). GIS and AHP techniques based delineation of groundwater potential zones: A case study from Southern Western Ghats, India. *Scientific Reports*, *9*(1), 2082. https://doi.org/10.1038/s41598-019-38567-x

Asaad, B. I., & Abed, B. Sh. (2020). Flow characteristics of Tigris River within Baghdad City during drought. *Journal of Engineering*, *26*(3), 77–92. https://doi.org/10.31026/j.eng.2020.03.07

Aykut, T. (2021). Determination of groundwater potential zones using Geographical Information Systems (GIS) and Analytic Hierarchy Process (AHP) between Edirne-Kalkansogut (northwestern Turkey). *Groundwater for Sustainable Development*, *12*, 100545. https://doi.org/10.1016/j.gsd.2021.100545

Bierkens, M. F. P., & Wada, Y. (2019). Non-renewable groundwater use and groundwater depletion: A review. *Environmental Research Letters*, *14*(6), 063002. https://doi.org/10.1088/1748-9326/ab1a5f

Chen, W., Li, H., Hou, E., Wang, S., Wang, G., Panahi, M., Li, T., Peng, T., Guo, C., Niu, C., Xiao, L., Wang, J., Xie, X., & Ahmad, B. B. (2018). GIS-based groundwater potential analysis using novel ensemble weights-of-evidence with logistic regression and functional tree models. *Science of The Total Environment*, *634*, 853–867. https://doi.org/10.1016/j.scitotenv.2018.04.055

Das, S., & Pardeshi, S. D. (2018). Integration of different influencing factors in GIS to delineate groundwater potential areas using IF and FR techniques: A study of Pravara basin, Maharashtra, India. *Applied Water Science*, *8*(7), 197. https://doi.org/10.1007/s13201-018-0848-x

Dawood, A., Jabbar, M., Gatea, M., & Al-Tameemi, H. (2018). A study of groundwater characteristics by using of groundwater quality index and pollution index in Zubair District, Basra Province, Iraq. *Journal of Applied Engineering Sciences*, *8*(21), 19–26. https://doi.org/10.2478/jaes-2018-0003

Etikala, B., Golla, V., Li, P., & Renati, S. (2019). Deciphering groundwater potential zones using MIF technique and GIS: A study from Tirupati area, Chittoor District, Andhra Pradesh, India. *HydroResearch*, *1*, 1–7. https://doi.org/10.1016/j.hydres.2019.04.001

Faroon, M. A., Yaseen, D. A., & Al Saad, Z. A. A. (2023). A new modeled equation of the water quality index for examination of the water quality of treatment plants in Basra City (Iraq). *Environmental Research, Engineering and Management*, *79*(1), 110–121. https://doi.org/10.5755/j01.erem.79.1.32707

Food and Agriculture Organization of the United Nations (FAO). (2003). *Digital soil map of the world and derived soil properties* [Map] (Version 3.6). https://www.fao.org/soils-portal/data-hub/soil-maps-and-databases/en/

Ghorbani Nejad, S., Falah, F., Daneshfar, M., Haghizadeh, A., & Rahmati, O. (2016). Delineation of groundwater potential zones using remote sensing and GIS-based data-driven models. *Geocarto International*, 1–21. https://doi.org/10.1080/10106049.2015.1132481

Greenbaum, D. (1992). Structural influences on the occurrence of groundwater in SE Zimbabwe. *Geological Society, London, Special Publications*, *66*(1), 77–85. https://doi.org/10.1144/GSL.SP.1992.066.01.04

Hindiyeh, M., Albatayneh, A., & AlAmawi, R. (2023). Water energy food nexus to tackle future Arab countries water scarcity. *Air, Soil and Water Research*, *16*, 11786221231160906. https://doi.org/10.1177/11786221231160906

Hussain, T. A., Almallah, I. A., & Qurnawi, W. S. A. (2021). Assessment of Dibdibba groundwater quality using the multivariate statistical technique in Zuber area south of Iraq. *Iraqi Journal of Science*, 2995–3008. https://doi.org/10.24996/ijs.2021.62.9.15

Ifediegwu, S. I. (2022). Assessment of groundwater potential zones using GIS and AHP techniques: A case study of the Lafia district, Nasarawa State, Nigeria. *Applied Water Science*, *12*(1), 10. https://doi.org/10.1007/s13201-021-01556-5

Iraqi Meteorological Organization and Seismology (IMOS). (2024). *Annual rainfall data (in millimeters) from 2006 to 2024* [Unpublished raw data]. Ministry of Transport.

Jassim, S. Z., & Goff, J. C. (Eds.). (2006). *Geology of Iraq* (1st ed.). Dolin; Moravian Museum.

Jha, M. K., Chowdary, V. M., & Chowdhury, A. (2010). Groundwater assessment in Salboni Block, West Bengal (India) using remote sensing, geographical information system and multi-criteria decision analysis techniques. *Hydrogeology Journal*, *18*(7), 1713–1728. https://doi.org/10.1007/s10040-010-0631-z

Jones, E. R., Van Vliet, M. T. H., Qadir, M., & Bierkens, M. F. P. (2021). Country-level and gridded estimates of wastewater production, collection, treatment and reuse. *Earth System Science Data*, *13*(2), 237–254. https://doi.org/10.5194/essd-13-237-2021

Lall, U., Josset, L., & Russo, T. (2020). A snapshot of the world's groundwater challenges. *Annual Review of Environment and Resources*, *45*(1), 171–194. https://doi.org/10.1146/annurev-environ-102017-025800

Leduc, C., Favreau, G., & Schroeter, P. (2001). Long-term rise in a Sahelian water-table: The Continental Terminal in South-West Niger. *Journal of Hydrology*, *243*(1–2), 43–54. https://doi.org/10.1016/S0022-1694(00)00403-0

Machiwal, D., Jha, M. K., & Mal, B. C. (2011). Assessment of groundwater potential in a semi-arid region of India using remote sensing, GIS and MCDM techniques. *Water Resources Management*, *25*(5), 1359–1386. https://doi.org/10.1007/s11269-010-9749-y

Mahdi, Z. H. A., & Hamdan, A. N. A. (2022). GIS-based analysis of water quality deterioration of the water treatment plants' effluents in Basrah province. *AIP Conference Proceedings*, *2386*(1), 040004. https://doi.org/10.1063/5.0066809

Malczewski, J. (1999). *GIS and multicriteria decision analysis*. J. Wiley.

Mawat, M. J., & Hamdan, A. N. A. (2024). 2D hydrodynamic and eutrophication modeling in the Shatt Al-Arab River, Basrah, Iraq. *Environmental and Earth Sciences Research Journal*, *11*(01), 1–19. https://doi.org/10.18280/eesrj.110101

Mekonnen, M. M., & Hoekstra, A. Y. (2016). Four billion people facing severe water scarcity. *Science Advances*, *2*(2), e1500323. https://doi.org/10.1126/sciadv.1500323

Metwally, A. B. M., Yasser, M. M., & Ahmed, M. (2024). Water for food in Euphrates–Tigris River. *Economies*, *12*(5), 107. https://doi.org/10.3390/economies12050107

Mukherjee, I., & Singh, U. K. (2020). Delineation of groundwater potential zones in a drought-prone semi-arid region of east India using GIS and analytical hierarchical process techniques. *CATENA*, *194*, 104681. https://doi.org/10.1016/j.catena.2020.104681

Mukherjee, P., Singh, C. K., & Mukherjee, S. (2012). Delineation of groundwater potential zones in arid region of India—A remote sensing and GIS approach. *Water Resources Management*, *26*(9), 2643–2672. https://doi.org/10.1007/s11269-012-0038-9

Ozegin, K. O., & Ilugbo, S. O. (2024). A triangulation approach for groundwater potential evaluation using geospatial technology and multi-criteria decision analysis (MCDA) in Edo State, Nigeria. *Journal of African Earth Sciences*, *209*, 105101. https://doi.org/10.1016/j.jafrearsci.2023.105101

Pinto, D., Shrestha, S., Babel, M. S., & Ninsawat, S. (2017). Delineation of groundwater potential zones in the Comoro watershed, Timor Leste using GIS, remote sensing and analytic hierarchy process (AHP) technique. *Applied Water Science*, *7*(1), 503–519. https://doi.org/10.1007/s13201-015-0270-6

Pradhan, R. M., Guru, B., Pradhan, B., & Biswal, T. K. (2021). Integrated multi-criteria analysis for groundwater potential mapping in Precambrian hard rock terranes (North Gujarat), India. *Hydrological Sciences Journal*, *66*(6), 961–978. https://doi.org/10.1080/02626667.2021.1906427

Saaty, T. L. (1980). *The analytic hierarchy process: Planning, priority setting, resource allocation*. McGraw-Hill International Book Company.

Sander, P., Chesley, M. M., & Minor, T. B. (1996). Groundwater assessment using remote sensing and GIS in a rural groundwater project in Ghana: Lessons learned. *Hydrogeology Journal*, *4*(3), 40–49. https://doi.org/10.1007/s100400050086

Saranya, T., & Saravanan, S. (2020). Groundwater potential zone mapping using analytical hierarchy process (AHP) and GIS for Kancheepuram District, Tamilnadu, India. *Modeling Earth Systems and Environment*, *6*(2), 1105–1122. https://doi.org/10.1007/s40808-020-00744-7

Saravanan, S., Saranya, T., Abijith, D., Jacinth, J. J., & Singh, L. (2021). Delineation of groundwater potential zones for Arkavathi sub-watershed, Karnataka, India using remote sensing and GIS. *Environmental Challenges*, *5*, 100380. https://doi.org/10.1016/j.envc.2021.100380

Shinde, S. P., Barai, V. N., Gavit, B. K., Kadam, S. A., Atre, A. A., Pande, C. B., Pal, S. C., Radwan, N., Tolche, A. D., & Elkhrachy, I. (2024). Assessment of groundwater potential zone mapping for semi-arid environment areas using AHP and MIF techniques. *Environmental Sciences Europe*, *36*(1), 87. https://doi.org/10.1186/s12302-024-00906-9

Todd, D. K., & Mays, L. W. (2005). *Groundwater hydrology* (3rd ed.). John Wiley & Sons. https://www.scribd.com/document/530473687/todd-Mays

U.S. Geological Survey. (2014). *Shuttle radar topography mission (SRTM) 1 arc-second global* [Dataset]. https://doi.org/10.5066/F7PR7TFT

U.S. Geological Survey. (2024). *Landsat 8 operational land imager (OLI) and thermal infrared sensor (TIRS) level-2 surface reflectance* [Dataset]. https://earthexplorer.usgs.gov

Yeh, H.-F., Cheng, Y.-S., Lin, H.-I., & Lee, C.-H. (2016). Mapping groundwater recharge potential zone using a GIS approach in Hualian River, Taiwan. *Sustainable Environment Research*, *26*(1), 33–43. https://doi.org/10.1016/j.serj.2015.09.005

Ying, X., Zeng, G.-M., Chen, G.-Q., Tang, L., Wang, K.-L., & Huang, D.-Y. (2007). Combining AHP with GIS in synthetic evaluation of eco-environment quality—A case study of Hunan Province, China. *Ecological Modelling*, *209*(2–4), 97–109. https://doi.org/10.1016/j.ecolmodel.2007.06.007

Zhu, Q., & Abdelkareem, M. (2021). Mapping groundwater potential zones using a knowledge-driven approach and GIS analysis. *Water*, *13*(5), 579. https://doi.org/10.3390/w13050579